

Accepted Manuscript

Benzimidazole acrylonitriles as multifunctional push-pull chromophores: Spectral characterisation, protonation equilibria and nanoaggregation in aqueous solutions

Ema Horak, Robert Vianello, Marijana Hranjec, Svjetlana Krištafor, Grace Karminski Zamola, Ivana Murković Steinberg



PII: S1386-1425(17)30099-9
DOI: doi: [10.1016/j.saa.2017.02.011](https://doi.org/10.1016/j.saa.2017.02.011)
Reference: SAA 14933

To appear in: *Spectrochimica Acta Part A: Molecular and Biomolecular Spectroscopy*

Received date: 28 October 2016
Revised date: 31 January 2017
Accepted date: 4 February 2017

Please cite this article as: Ema Horak, Robert Vianello, Marijana Hranjec, Svjetlana Krištafor, Grace Karminski Zamola, Ivana Murković Steinberg, Benzimidazole acrylonitriles as multifunctional push-pull chromophores: Spectral characterisation, protonation equilibria and nanoaggregation in aqueous solutions. The address for the corresponding author was captured as affiliation for all authors. Please check if appropriate. Saa(2017), doi: [10.1016/j.saa.2017.02.011](https://doi.org/10.1016/j.saa.2017.02.011)

This is a PDF file of an unedited manuscript that has been accepted for publication. As a service to our customers we are providing this early version of the manuscript. The manuscript will undergo copyediting, typesetting, and review of the resulting proof before it is published in its final form. Please note that during the production process errors may be discovered which could affect the content, and all legal disclaimers that apply to the journal pertain.

**Benzimidazole acrylonitriles as multifunctional push-pull
chromophores: spectral characterisation, protonation
equilibria and nanoaggregation in aqueous solutions**

Ema Horak^a, Robert Vianello^b, Marijana Hranjec^c, Svjetlana Krištafor^a, Grace Karminski
Zamola^c and Ivana Murković Steinberg^{a*}

*^aDepartment of General and Inorganic Chemistry, Faculty of Chemical Engineering and Technology,
University of Zagreb, Marulićev trg 19, HR 10000 Zagreb, Croatia*

*^bComputational Organic Chemistry and Biochemistry Group, Ruđer Bošković Institute, Bijenička
cesta 54, HR 10000 Zagreb, Croatia*

*^cDepartment of Organic Chemistry, Faculty of Chemical Engineering and Technology
University of Zagreb, Marulićev trg 20, HR 10000 Zagreb, Croatia*

*Corresponding author:

Ivana Murković Steinberg, Department of General and Inorganic Chemistry, Faculty of Chemical
Engineering and Technology, University of Zagreb, Marulićev trg 19, HR-10000 Zagreb, Croatia,
Phone No. ++38514597287; e-mail: ivana.murkovic@fkit.hr

Abstract

Heterocyclic donor- π -acceptor molecular systems based on an *N,N*-dimethylamino phenylacrylonitrile benzimidazole skeleton have been characterised and are proposed for potential use in sensing applications. The benzimidazole moiety introduces a broad spectrum of useful multifunctional properties to the system including electron accepting ability, pH sensitivity and compatibility with biomolecules. The photophysical characterization of the prototropic forms of these chromophores has been carried out in both solution and on immobilisation in polymer films. The experimental results are further supported by computational determination of pK_a values. It is noticed that compound **3** forms nanoaggregates in aqueous solutions with aggregation-induced emission (AIE) at 600 nm. All the systems demonstrate spectral pH sensitivity in acidic media which shifts towards near-neutral values upon immobilisation in polymer films or upon aggregation in an aqueous environment (compound **3**). The structure-property relationships of these functional chromophores, involving their spectral characteristics, acid-base equilibria, pK_a values and aggregation effects have been determined. Potential applications of the molecules as pH and biomolecular sensors are proposed based on their pH sensitivity and AIE properties.

Keywords: push-pull chromophores; benzimidazole; aggregation induced emission (AIE); pH sensitivity; prototropic equilibrium

1. Introduction

Intramolecular charge-transfer (ICT) organic systems based on electron donor- π -bridge-electron acceptor structures (D- π -A) are widely used as chromophores and fluorophores in advanced functional materials [1] and (bio)analytical or imaging applications [2].

The photophysical and chemical properties of such push-pull molecular systems are defined by the position, number and electron donating and accepting strengths of donor and acceptor groups and their chemical nature. Insight into the structure-property relationships allows fine tuning of their functional properties [3-5]. In this respect D- π -A systems based on heteroaromatic scaffolds such as styryl heterocycles [6-8] or imidazole derivatives [9] are especially interesting due to the additional functional molecular features they bring to chromophores: specific chemical and biological activity.

The benzimidazole moiety (BI) can serve as a multifunctional unit in such heteroaromatic molecular systems: its electron accepting and π bridging properties combined with chromogenic pH sensitivity/switching, metal-ion chelating properties and compatibility with biomolecules makes the BI moiety an especially attractive building block in D- π -A systems for different applications: optoelectronics and non-linear optics (NLO), photovoltaics, sensing and bioimaging. Representative examples of BI based ICT chromo- and fluorophores include materials for OLEDs [10], dye-sensitised solar cells (DSSCs) [11, 12] and molecular chemosensors [13], sensors for pH [14-17] metal-ions [18, 19], anions [20], biomolecules [21], and pH probes for bioimaging [22].

The structure-property impact of BI units within D- π -A heteroaromatic chromophores, especially pH sensitivity, has been studied in detail spectroscopically and theoretically [23-26] in potential sensing applications and for NLO pH switching. Studies involve computational prediction and determination of pK_a values and photophysical or non-linear

properties and usually represent the first step in the design of novel multi-responsive molecular systems.

As a result of their dipolar structure, the ICT compounds can also form self-assembled functional molecular systems [27]. The cyano group, as a typical strong electron acceptor in D- π -A systems strongly affects the spectral characteristics of the molecules (λ_{abs} and ϵ), as well as the basicity of neighbouring nitrogen atoms and their corresponding pK_a values [28]. Additionally, the presence of a cyano group in these chromophores has been identified as a key factor in the creation of supramolecular interactions [29-32], leading to the formation of fluorescent organic nanoparticles (FONs) that exhibit aggregation induced emission (AIE) [33]. Aggregation induced emission is a photophysical phenomenon with great application promise, related to certain organic molecules which exhibit stronger fluorescence in their aggregated states than in the dissolved state.

Here we present multifunctional D- π -A molecular systems containing an *N,N*-dimethylamino group as a pH sensitive donor group connected via a π linker (styryl) to the electron accepting substituents: cyano group and the pH sensitive benzimidazole moiety (Fig. 1).

Fig. 1.

The photophysical characterisation and computationally supported determination of species involved in prototropic equilibria, including their respective pK_a values, have been performed in order to better understand the effects of the D- π -A molecular structure on the UV-Vis spectral properties, nanoaggregation and pH sensing potential of these chromophores.

The results are critically evaluated in the light of structurally similar multifunctional compounds including cyanostilbenes [34], styrylbenzoxazoles [35] and cyanovinyl substituted

benzimidazoles [11, 19] as promising candidates for functional application as AIE-based pH probes, dye sensitizers in solar cells and as metal-ion sensors.

2. Materials and Methods

2.1. Reagents and instrumentation

Chemicals for synthesis and pure organic solvents were purchased from commercial suppliers Acros, Aldrich or Fluka. Hydrochloride acid and potassium hydroxide were obtained from Kemika d.d., Zagreb. Poly(vinylchloride) (PVC, high molecular weight) for thin film preparation was purchased from Fluka, whilst dioctyl sebacate (DOS) and potassium tetrakis(4-chlorophenyl)borate (PTCB) were obtained from Sigma-Aldrich. Polyester sheets (Laser + Copier Film 210 x 297 mm, $d = 0.1$ mm) were purchased from Zweckform. Milli-Q water was used for the preparation of aqueous solutions. pH was measured on commercially available pH electrode Blue Line 17 pH, Schott AG, Mainz, Germany. Absorption spectra were recorded by Cary 100 Scan Varian spectrophotometer. Fluorescence measurements were carried out by Varian Cary Eclipse fluorescence spectrophotometer. Quartz cells of 1 cm path length were used throughout measurements and absorbance and fluorescence values were recorded at 1 nm. Wavelength scan was performed between 250 nm and 800 nm. Baseline was recorded prior to each set of experiments in aqueous and non-aqueous solutions. Emission spectra corrected for the effects of time- and wavelength-dependent light-source fluctuations using a standard of Rhodamine 101, a diffuser provided with the fluorimeter and the software supplied with the instrument. Dynamic light scattering (DLS) experiments were conducted using Malvern Zetasizer Nano range light scattering instrument.

2.2. Synthesis of benzimidazole derivatives

All chemicals and solvents were purchased from commercial suppliers Aldrich and Acros. Melting points were recorded on SMP11 Bibby and Büchi 535 apparatus. NMR spectra were measured in DMSO- d_6 solutions using TMS as an internal standard. The ^1H and ^{13}C NMR spectra were recorded on a Varian Gemini 300 or Varian Gemini 600 at 300, 600 and 150 and 75 MHz, respectively. Chemical shifts are reported in ppm (δ) relative to TMS. All compounds were routinely checked by TLC with Merck silica gel 60F-254 glass plates. The 2-benzimidazolyl substituted chromophores **1-4** (Fig. 2) were prepared in one-step condensation of 2-cyanomethylbenzimidazole or 2-cyanomethyl-*N*-phenylbenzimidazole with corresponding heteroaromatic aldehydes in absolute ethanol by adding a few drops of piperidine [19, 36]. Detailed synthesis and structure properties of **1-4** can be found in supplementary material.

Fig. 2.

2.3. Photophysical characterisation and acid-base properties

Basic photophysical properties of examined compounds were characterised by UV-visible absorption and fluorescence spectroscopy. Spectra were recorded in solvents with different $E_{\text{T}}(30)$ solvent polarity parameters [37]. The concentration of the chromophore solutions was 1×10^{-5} mol dm^{-3} . All the solvents were of high purity grade. Excitation wavelengths were determined from absorbance maxima. Quantum yields were determined by IUPAC method using quinine sulphate as standard ($\Phi = 0.546$). The characterisation of benzimidazole derivatives **1-4** was conducted by diluting the stock solutions in methanol or ethanol (methanol or ethanol volume fraction in diluted solutions did not exceed 1.5 %).

Concentrations of stock solutions were as it follows: $c(\mathbf{1})=2.18\times 10^{-3}$ mol dm⁻³; $c(\mathbf{2})=1.35\times 10^{-3}$ mol dm⁻³ $c(\mathbf{3})=6.4\times 10^{-4}$ mol dm⁻³; $c(\mathbf{4})=9.2\times 10^{-4}$ mol dm⁻³.

The pH titration experiments were carried out using 1×10^{-5} mol dm⁻³ solutions of the compounds **1-4** in 0.1 M hydrochloric acid or 0.1 M potassium hydroxide solutions. The adjustment of pH was achieved through the acid or base addition until the change of pH within 0.5 units occurred. Following each addition of titrant, UV-visible absorption spectrum was recorded after the time required keeping the drift of pH electrode within 0.1 pH units per minute. Titrations were conducted at constant ionic strength $I = 0.1$ M, in potassium chloride solutions. The pK_a values were calculated as the x-coordinate of the inflection point of the Boltzmann function (1) obtained from spectrophotometric titrations data:

$$y = \frac{A_1 - A_2}{1 + e^{(x - x_0)/dx}} + A_2 \quad (1)$$

Dynamic light scattering (DLS) experiments were carried out in aqueous ($f_w = 99\%$ water/ethanol) and in ethanol solution, $c = 10$ μ M.

2.4. Theoretical calculations of pK_a values

All of the molecular geometries were initially optimised in the gas-phase by the efficient and accurate M06-2X/6-31+G(d,p) model. The thermal corrections were extracted from the corresponding frequency calculations without the application of scaling factors. The final single-point energies were attained with a highly flexible 6-311++G(2df,2pd) basis set using the MP2 approach giving the MP2/6-311++G(2df,2pd)//M06-2X/6-31+G(d,p) model employed here for the gas-phase free energies. To account for the solvation effects, we reoptimized geometries employing the SMD polarisable continuum model [38] at the (SMD)/M06-2X/6-31+G(d,p) level with all parameters corresponding to pure water, and

calculated solvation free energies as a difference between the corresponding SMD and gas-phase calculations at the same level of theory. The choice of such a computational setup was prompted by our success in estimating both pK_a and reaction thermodynamic values in solution [39, 40]. pK_a values were calculated in a relative fashion using $AH + B_{REF} \rightarrow A^- + B_{REF}H$ equation, and employing the following reference bases ($B_{REF}H$): benzimidazole ($pK_a = 12.75$ and 5.41) [41] for the deprotonation and protonation of this fragment, respectively, and *N,N*-dimethylaniline ($pK_a = 5.15$) [41] for the protonation of the dimethylamino group in investigated systems. All of the calculations were performed using the Gaussian 09 software [42].

2.5. Immobilisation of 3-4 in polymer films

Chromophores **3** and **4** were immobilised in plasticised PVC matrix starting from liquid mixture prepared by modified published method [43]. The "cocktail" contained 67 mg PVC, 134 mg DOS (the plasticiser), 2.4 mg (1 eq) of PTCB and 1 eq of compound **3** or **4** in 1.5 mL THF. Mixture was placed in ultrasonic bath for 15 min. Thin polymer films were prepared by spreading 100 μ L mixture onto a 2.5 x 2.5 cm solid transparent polyester sheet by spin-coating technique. Obtained thin films were dried at room temperature for 18 h in dark. pH response of immobilised chromophores was examined in buffer solutions, pH 2 to 12.

2.6. DNA interaction experiments

A polynucleotide calf thymus DNA was purchased from Sigma and Aldrich, and used without further purification. Polynucleotide was dissolved in the BPE buffer (6mM Na_2HPO_4 , 2mM NaH_2PO_4 , 1mM EDTA), pH=7.0. Stock solution of compound **3** was prepared in ethanol. Respective aliquot of stock solution of **3** was added to the aqueous buffer ($c = 1 \times 10^{-5}$ mol dm^{-3}) and titration with DNA was conducted.

Spectral measurements were performed in aqueous buffer solution (BPE buffer, pH=7.0, and phosphate buffer, pH = 7.4). Absorbance and emission spectra were recorded after every addition of DNA aliquot. The partial volume of ethanol in water did not exceed 0.1%.

3. Results and Discussion

3.1. Design and D- π -A structure of chromophores

Compounds **1** and **2** as parent molecules were converted into D- π -A molecular systems (compounds **3** and **4**) by introduction of strong electron donating *N,N*-dimethylamino group, (D) into their phenylacrylonitrile benzimidazole conjugated skeleton.

Fig. 3.

In terms of D- π -A arrangement the structures of chromophores **3** and **4** are shown in Fig. 3. In compound **3** the $-\text{NMe}_2$ as a strong donor group (D) is connected via π linker (styryl) to the very strong acceptor group A1 (cyano) and a weaker acceptor A2 (benzimidazole unit) forming a D- π -A1-A2 structure. In compound **4**, the benzimidazole moiety is modified with bulky electron donating phenyl substituent (D1) which increases the electron density of A2.

All structures contain acid-base active sites as a part of either donor or acceptor moiety and are marked in Fig. 3. These are amino nitrogen atom (in donor group D) and imino (azole) nitrogen atom (in acceptor group A2) as protonable sites in **3** and **4**. The NH group on the benzimidazole ring in **3** is marked as deprotonable site.

Structural analogues of **3** previously reported in the literature included *N,N*-dimethylamino styryl benzimidazole [25] (D- π -A2), *N,N*-dimethylamino pyridyl acrylonitrile [32] (D- π -A1-

pyridyl), cyanostilbene derivatives [34] (D- π -A1-(phenyl or phenoyl)) and *N,N*-diethylamino analogue of **3** with carboxyl group attached to BI moiety [11].

The proposed donor- π - acceptor structures were used as a basis for discussion of structure-property relationships of **1-4** determined in this study (photophysical properties of prototropic species and the corresponding pK_a values).

3.2. Photophysical properties of chromophores 1-4

The chromophores were studied by UV-Vis absorption and fluorescence spectroscopy in different solvents. Absorption spectra of compounds **1-4** in ethanol are shown in Fig. 4a, and their basic photophysical properties in ethanol are summarised in Table 1.

Fig. 4.

Table 1.

Compounds **1** and **2** show the main absorption bands with maxima at 350 nm and 335 nm respectively. As expected, introduction of an *N,N*-dimethylamino group ($-NMe_2$) into **1** and **2** caused a bathochromic shift of 75 nm and 65 nm and considerable increase of molar absorption coefficients, as observed in compounds **3** and **4**, respectively (Table 1).

Both effects can be explained by the appearance of a strong intramolecular charge transfer (ICT) due to D-A interactions involving the electron donating $-NMe_2$ group.

As a result of its D- π -A1-A2 structure with enhanced push-pull effects, compound **3** shows the greatest red-shift with an absorption maximum at 425 nm, and a very high molar absorption coefficient of $43\,910\text{ dm}^3\text{ cm}^{-1}\text{ mol}^{-1}$. In **4**, ICT effects are less pronounced due to D- π -A1-A2-D1 structure in which the electron donating phenyl substituent (D1) reduces the electron accepting power of the acceptor moiety. Previously reported *N,N*-dimethylamino styryl benzimidazole [25] has an absorption maximum at 374 nm. Introduction of a strong

electron-withdrawing cyano group into its skeleton (compound **3**) results in a 50 nm bathochromic shift. All compounds show modest fluorescence in ethanol with quantum yields less than 0.01 and emission maxima that range from 444 nm to 491 nm. Due to relatively low fluorescence intensity in ethanol the compounds are not readily promising candidates for fluorimetric analytical applications.

The absorption spectra of **1-4** in aqueous solutions are shown in Fig. 4b, and the summary of absorption spectroscopy data in solvents of different polarity are presented in Table 2.

The absorption maxima of compounds **1** and **2** (λ_{abs}) recorded in solvents of varying polarity indicate a weak negative solvatochromic effect. A change of solvent from toluene to water induced a blue-shift in the absorption maxima of $\Delta\lambda(\mathbf{1}) = 18$ nm and $\Delta\lambda(\mathbf{2}) = 10$ nm. Compound **3** in water showed unusual spectral characteristics (Fig. 4b) indicating the presence of specific solvent effects, whilst **4** exhibited a very small positive solvatochromism with absorption maxima ranging from 390 nm in nonpolar aprotic toluene to 400 nm and 404 nm in hydrogen bond donating solvents, ethanol/methanol and water respectively. The reason for the different solvatochromic responses of **1-4** is most likely due to their different D-A structures, position and nature of ionisable sites (Fig. 3), and the corresponding polarity of the molecules in their respective ground and excited states. The small blue shift observed in **1** and **2** on increased solvent polarity suggests that these molecules possess a greater dipole moment in their ground state than in their respective excited states, whereas the red shift of **4** can be explained by a greater dipole moment in the excited state, leading to stronger stabilisation in solvents of higher polarity. A similar trend is observed for molar absorption coefficients (ϵ) which generally decrease on going from toluene to water for **3** and **4**. The spectral bandwidth expressed as FWHM (Full Width at Half Maximum) value is fairly constant for **1** and **2** in all solvents (around 70 nm), but for **3** (except in water) and **4** increases with solvent polarity, as shown in Table 2. In comparison with other compounds, **3** has the highest values of ϵ and λ_{abs}

in all solvents (except in water), which can be attributed to its stronger ICT character as discussed earlier based on its D- π -A1-A2 structure.

Table 2.

It is evident that compound **3** show significantly different spectral characteristics in water in comparison to other solvents. Namely, **3** is yellow in all solvents except in water. Water solution is visually colourless and transparent, and spectrally it shows a sharp non-symmetrical (red-tailed) absorption band (FWHM value of 31 nm) with a maximum at around 350 nm (Fig. 4b). The water solution absorption peak wavelength λ_{abs} of **3** is blue-shifted by approximately 70 nm in comparison to other solvents. The ICT character of **3** becomes less pronounced in water solutions and is comparable to the spectral characteristics of compound **1**, its non-ICT analogue. These findings strongly indicate the presence of dye nanoaggregates, formed by the specific intermolecular interactions in aqueous environment. The shape of the absorption spectrum of **3** in water indicates presence light scattering effects on nanoparticles [44]. This was confirmed by Tyndall effect which occurred on visually transparent solution of **3** using a laser beam, as shown in Fig. S1A. In addition, the presence of nanometer and micrometer sized aggregates of **3** in aqueous solutions ($f_w = 99\%$, $c = 10\ \mu\text{M}$) was confirmed by dynamic light scattering experiments (Fig S1B).

It was also noticed that the water solution of **3** (colourless under ambient light) shows orange-red emission under UV light. Hence, the effects of nanoaggregation on spectroscopic properties of **3** were further studied in mixed solvent solutions (water-ethanol).

3.3. Aggregation induced emission in aqueous solutions

The absorption and emission characteristics of **3** were investigated in water-ethanol mixtures of varying volume fraction of water, f_w . The resulting spectra are shown in Fig. 5a.

Fig. 5.

Compound **3** shows orange-red fluorescence emission at 600 nm in water, which gradually disappears upon addition of ethanol (Fig. 5). At a water fraction of $f_w = 0.80$ virtually no fluorescence emission at 600 nm is observable. The intensity of orange emission in aqueous solution ($f_w = 99\%$) is approximately 35-fold the emission in ethanol at 600 nm. This photophysical phenomenon can be explained by aggregation induced emission, as first reported by Tang *et al.* [45] and Park *et al.* [30]. Unlike most organic fluorophores, some organic molecules exhibit strong fluorescence upon aggregation in poor solvents or in the solid-state. Different mechanisms have been proposed to explain AIE including restriction of intramolecular rotation (RIR), J-aggregate formation, twisted intramolecular charge transfer (TICT) and others [33].

Since a previously reported analogue of **3**, *N,N*-dimethylamino styryl benzimidazole [25], does not show aggregation in water, it is clear that the presence of the cyano group in **3** is responsible for intermolecular changes leading to the observed AIE. It is known that supramolecular interactions, especially hydrogen bonds and other dipole-dipole interactions involving cyano groups [46] may be responsible for the suppression of intramolecular motions in crystals resulting in tight molecular arrangements of increased rigidity leading to AIE phenomena [32, 47]. However, compound **4** also contains a cyano group but does not show aggregation in water. The BI moiety in **4**, with its bulky electron donating phenyl substituent (D1), disturbs the molecular planarity and prevents certain dipole-dipole interactions that are possibly responsible for the aggregation observed in compound **3**. It is interesting to note that the observed blue-shift in the absorption band of **3** on going from ethanol (440 nm) to aqueous solution (350 nm) can easily be associated with the formation of non-emissive H-aggregates resulting from π -stacking interactions. However, in contrast to

that, **3** shows red-shifted and significantly increased emission in nanoaggregated form. This can be related to a less common conformation of emissive H-aggregates [48] where the presence of the bulky and polar cyano group is known to affect the parallel face-to-face intermolecular interactions [30].

3.3. Protonation equilibria and pK_a values

3.3.1. Protonated species of 1-4 in ethanol

In order to define the species involved in neutral–monocation equilibria, spectral characterisation was first performed in acidified ethanol solutions to avoid possible complications due to observed nanoaggregation in aqueous solutions.

Absorption and emission spectra of neutral (M) and monoprotonated species (M^+) of **1-4** are shown in Fig. 6 and the summary of spectral properties of neutral and protonated chromophores in ethanol are presented in Table S1. Excitation and emission spectra of **3** and **4**, in neutral and protonated forms in ethanol, are shown in Fig. S2.

Fig. 6.

The absorption spectra of protonated species of compounds **1** and **2** in ethanol (Fig. 6) show no significant change of the longest wavelength peak, whilst compounds **3** and **4** exhibit bathochromic shifts with increased extinction coefficients. Since monoprotonated species of **3** and **4** contain two protonable sites (*N,N*-dimethylamino nitrogen and imino nitrogen on BI moiety) the question is which nitrogen atom is more basic and would be protonated first.

It is generally known that protonation of a donor group (amino) in a push-pull system is reducing its electron-donating character and decreasing conjugation which results in a blue shift of the absorption spectrum and decreased extinction coefficient. On the other hand,

protonation of acceptor moiety in a push-pull system is enhancing acceptor's electron-withdrawing character and results in a red-shift and increased extinction coefficients of molecules. The spectroscopic results indicate that protonation in **3** and **4** occurs first on imino nitrogen atom on BI moiety (the acceptor group), which is in agreement with previously reported styryl analogue of **3** [25] and the hydrochloride monohydrate of **3** whose crystal structure also confirmed that protonation occurs on imino nitrogen [36]. This is further corroborated by the computational results presented later.

Protonation of BI moiety on **1** and **2** (which are not typical ICT molecules) is not related to significant changes in absorption spectra. The lone electron pair on imino nitrogen occupies sp^2 hybrid orbital and is not involved in the π electron system. Its protonation does not considerably affect HOMO-LUMO energy levels, so the absorption spectra remain virtually unchanged. Fluorescence emission of neutral species in ethanol is relatively weak (Table 1). Protonation of **1** and **2** leads to increased fluorescence emission without shift of emission wavelength.

3.3.2. Spectroscopic pH titrations of 1-4 in aqueous solutions

General protonation-deprotonation equilibria and corresponding pK_a values of compounds **1-4** are shown in Scheme 1. (Note: under investigated conditions compounds **1** and **2** do not form M^{2+} species, while compounds **2** and **4** do not form M^- species)

Scheme 1.

The spectroscopic pH titrations were performed in aqueous solutions in the pH range 1.5 to 13.0 and the resulting absorption spectra for **3** and **4** are shown in Fig. 7a and 7b, respectively. The spectral identification of all species involved in respective protonation-deprotonation

equilibria of **1-4** in aqueous solutions was performed, and the summary of spectroscopic properties is presented in Table S2. Spectral properties of dicationic and anionic (deprotonated) species are estimated from spectra obtained at pH = 1.0 and pH = 14.0, respectively.

As shown in Fig. 7a titration spectra of **3** show three distinct pH ranges corresponding to: i) protonation of neutral form (pH range 1.5 to 5); ii) neutral form (aggregate) at pH values ranging from approximately 5 to 8, and iii) deprotonation of neutral form (pH range 9 to 13). The protonation of monoprotonated form to dication form (amino-protonated species) occurs at pH values below 2 and is accompanied with blue shifted absorption maxima at 335 nm. The pH titration spectra of **4** show no evidence of aggregation and correspond to equivalent spectra obtained in ethanolic solutions.

Monoprotonated forms of both, **3** and **4** have considerably higher molar extinction coefficients than the corresponding neutral species, as expected from their ICT structure since protonation occurs at the acceptor moiety.

Fig. 7.

3.3.3. Experimental and theoretical pK_a values in aqueous solutions

The pK_a values are experimentally determined or estimated from spectroscopic titration data. Fig. 8 shows examples of plots used for experimental determination of pK_a values.

Fig. 8.

In order to rationalize the acid/base features of studied systems in aqueous solution we performed a computational analysis employing the implicit SMD solvation. The calculated

pK_a values (Table 3) show remarkable agreement with experimental data, which lends credence to the applied computational model. In comparison with the six precisely measured values, the average absolute deviation is only 0.6 pK_a units, which is remarkable for this kind of calculations. Nevertheless, we must emphasize that it would be even much lower if it would not include a 2 pK_a difference in the $pK_{a2}(\mathbf{3})$ value that we attribute to the reported aggregation of this system in water, which complicates experimental pK_a determination.

Table 3.

Interestingly, the first protonation of all four systems **1–4** occurs on the benzimidazole imino nitrogen. This might be expected considering that benzimidazole ($pK_a = 5.41$) is slightly more basic than *N,N*-dimethylaniline ($pK_a = 5.07$) [41], together with the fact that the cyano group in **3** and **4** is in a direct resonance interaction with the latter fragment, thus reducing its basicity. In the parent system **1**, imino nitrogen protonation is associated with $pK_{a2} = 3.0$ making it significantly less basic than benzimidazole. This is a general trend in all **1–4**, which strongly indicates that under normal conditions all four investigated systems are predominantly present as unionized neutral molecules, which is a significant observation. We attribute this trend to the presence of the electron withdrawing styryl moiety, which diminishes the basicity of the benzimidazole fragment. This effect is slightly compensated by adding the electron donating $-NMe_2$ group in **3** and **4**, where the corresponding pK_{a2} values increase to 4.2 and 3.7, but still not enough to make these systems more basic than benzimidazole. As expected, if we remove the strongly acidifying cyano group [49, 50] from **1** (model system **I**, Table 3) the corresponding pK_a value increases to 5.8.

The second protonation of **3** and **4** occurs at the dimethylamino group and, interestingly, it requires only slightly stronger acids than those able to allow the corresponding monocations.

pK_{a1} values for **3** and **4** assume 1.1 and 2.0 (Table 3), which could be achieved with two equivalents of already moderately strong acids. As mentioned, dimethylamino positions are in a direct resonance with the attached cyano group, so these positions in **3** and **4** are significantly less basic than *N,N*-dimethylaniline ($pK_a = 5.07$). Differing effect of the $-CN$ group is evident in the changes of bond distances induced upon protonation. For example, after the imino protonation of **3** to $\mathbf{3}^+$, the C–N distance of the cyano group is not changed and remains the same at 1.162 Å, but is subsequently reduced to 1.159 Å after amino protonation of $\mathbf{3}^+$ to $\mathbf{3}^{2+}$. In line with previous discussion, dication \mathbf{I}^{2+} is even more easily attainable ($pK_{a1} = 3.3$). On the other hand, the unsubstituted benzimidazole amino groups in **1** and **3** are prone to deprotonation. Relative to benzimidazole deprotonation ($pK_a = 12.75$) [41], the presence of the cyano group increases the acidity of **1** and **3** by two orders of magnitude to the pK_{a3} values of 10.4 and 10.3 (Table 3), which is notable, yet not enough to make these systems monoanions under normal conditions. Since **1** is deprived of the cyano group, this effect is absent ($pK_{a3} = 12.5$).

In concluding this section, it is worth emphasizing that the calculations underline a significant electronic effect of the cyano group in affecting acid/base properties of **1-4**, and convincingly demonstrate that all investigated systems are neutral molecules under normal conditions, which become monoprotonated exclusively on the benzimidazole imino with moderately strong acids (pK_a values between 2 – 4).

The neutral species of **3** forms nanoaggregates in aqueous solution. The deaggregation process can be triggered either by protonation or deprotonation of molecules occurring at pH values lower than 5 or higher than 8, respectively. It is important to note that the aggregation-deaggregation process is reversibly switched by changing the pH of the aqueous solution, opening up interesting potential applications for compound **3** in AIE-based pH sensing and imaging. Also, it has previously been shown that the hydrochloride monohydrate of **3**

interacts with DNA molecules [36], a result which should now be explored further in light of the spectrally responsive and pH sensitive deaggregation processes we report here.

3.4. pH sensitivity of chromophores in polymer matrix

Thin polymer films based on plasticised PVC containing immobilised **3** and **4** were fabricated and initially tested as optically pH responsive materials for ion-selective optodes. The spectral and visual responses to pH, as well as the corresponding calibration plot of immobilised **3** are shown in Fig. 9.

Fig. 9.

Table 4.

Absorption and emission properties and the corresponding apparent pK_a values of neutral and monocation forms of immobilised **3** and **4** are summarised in Table S3. The spectral response of the immobilised chromophores corresponds to ethanolic solutions and no aggregation of **3** was noticed. The apparent pK_a values increased by nearly 3 pK_a units in comparison to their aqueous values. Such changes are expected due to a number of known parameters affecting the complex heterogeneous ion-exchange equilibria in ion-selective optodes [51].

3.5. Effect of DNA on aggregation

The effect of DNA on the aggregation/deaggregation equilibrium of **3** has been studied. The absorption and emission spectral responses obtained in a *ct*-DNA titration experiment are shown in Fig. 10. In the presence of DNA the absorbance and emission intensities of the nanoaggregated form of **3** (at 350 nm and 600 nm, respectively) decrease. The corresponding titration plot is shown (Fig. 10, inset). The interaction between **3** and the *ct*-DNA molecules

results in quenching of AIE. The interaction is most likely based on structural compatibility of the planar BI moiety and its ability to incorporate between adjacent base pairs of the DNA molecule during the intercalation process [36, 52].

Fig. 10.

4. Conclusion

The benzimidazole-based push-pull molecular systems presented in this work exhibit pH induced spectral responses in the visible region with relatively high molar absorption coefficients. In general, the fluorescence properties of the molecules are not promising for applications requiring high quantum yields, with the exception of **3** and the corresponding aggregation-induced emission. All the chromophores demonstrate pH sensitivity with pK_a values in acidic (2.1-3.0) and basic (around 10) ranges, corresponding to neutral-monocation and neutral-anion equilibria. Computational analysis aided in rationalising acid/base features of the systems investigated, and demonstrated that all compounds are unionised under normal conditions, but become monoprotonated exclusively on the benzimidazole imino nitrogen with only moderately strong acids (pK_a values between 2-4). However, the apparent pK_a values of **3** and **4** when immobilised in polymer films shifted to 6.3, enabling possible future application of these chromophores as physiologically compatible pH sensitive materials. An important finding is the ability of **3** to form emissive nanoaggregates in solution triggered by either solvent composition or the pH value of the aqueous solution. Its near-neutral pH-switchable aggregation/deaggregation is accompanied by absorption and emission changes making it promising for pH sensing and imaging applications. An additional advantage for

biological applications is the excitation at 350 nm resulting in a long wavelength emission at 600 nm.

Further studies exploring the effects of interactions of the BI moiety with biomolecules and metal-ions on AIE are underway in our laboratory.

Acknowledgments

This work was supported by the Croatian Science Foundation under grant number IP-2014-09-3386 entitled *Design and synthesis of novel nitrogen-containing heterocyclic fluorophores and fluorescent nanomaterials for pH and metal-ion sensing* which is gratefully acknowledged. We would like to thank Dr. Maja Dutour Sikirić and Dr. Darija Domazet Jurašin of Ruđer Bošković Institute, Zagreb, for use of the DLS instrumentation and for characterisation of the nanoaggregates. We would also like to thank Dr. Matthew D. Steinberg for reviewing the manuscript.

References

- [1] T.D. Kim, K.S. Lee, *Macromol. Rapid Commun.* 36 (2015) 943-958.
- [2] C. Barsu, R. Cheaib, S. Chambert, Y. Queneau, O. Maury, D. Cottet, H. Wege, J. Douady, Y. Bretonniere, C. Andraud, *Org. Biomol. Chem.* 8 (2010) 142-150.
- [3] Y.Z. Wu, W.H. Zhu, *Chem. Soc. Rev.* 42 (2013) 2039-2058.
- [4] F. Bures, *RSC Adv.* 4 (2014) 58826-58851.
- [5] L. Beverina, G.A. Pagani, *Acc. Chem. Res.* 47 (2014) 319-329.
- [6] S.L. Wang, T.I. Ho, *J. Photochem. Photobiol. A-Chem* 135 (2000) 119-126.

- [7] M. Zajac, P. Hrobarik, P. Magdolen, P. Foltinova, P. Zahradnik, *Tetrahedron* 64 (2008) 10605-10618.
- [8] Z. Seferoglu, H. Ihmels, E. Sahin, *Dyes Pigment.* 113 (2015) 465-473.
- [9] J. Kulhanek, F. Bures, *Beilstein J. Org. Chem.* 8 (2012) 25-49.
- [10] M.Y. Lai, C.H. Chen, W.S. Huang, J.T. Lin, T.H. Ke, L.Y. Chen, M.H. Tsai, C.C. Wu, *Angew. Chem.-Int. Edit.* 47 (2008) 581-585.
- [11] S. Manoharan, S. Anandan, *Dyes Pigment.* 105 (2014) 223-231.
- [12] G.M. Saltan, H. Dincalp, M. Kiran, C. Zafer, S.C. Erbas, *Mater. Chem. Phys.* 163 (2015) 387-393.
- [13] Y.C. Wu, J.Y. You, L.T. Guan, J. Shi, L. Cao, Z.Y. Wang, *Chin. J. Org. Chem.* 35 (2015) 2465-2486.
- [14] M.A. Saeed, H.T.M. Le, O.S. Miljanic, *Accounts Chem. Res.* 47 (2014) 2074-2083.
- [15] R.C. Lirag, H.T.M. Le, O.S. Miljanic, *Chem. Comm.* 49 (2013) 4304-4306.
- [16] Z.S. Li, L.J. Li, T.T. Sun, L.M. Liu, Z.G. Xie, *Dyes Pigment.* 128 (2016) 165-169.
- [17] R. Cinar, J. Nordmann, E. Dirksen, T.J.J. Muller, *Org. Biomol. Chem.* 11 (2013) 2597-2604.
- [18] M.M. Henary, Y.G. Wu, C.J. Fahrni, *Chem.-Eur. J.* 10 (2004) 3015-3025.
- [19] M. Hranjec, E. Horak, M. Tireli, G. Pavlovic, G. Karminski-Zamola, *Dyes Pigment.* 95 (2012) 644-656.
- [20] N. Singh, D.O. Jang, *Org. Lett.* 9 (2007) 1991-1994.
- [21] S.L. Wang, Y.T. Chang, *J. Am. Chem. Soc.* 128 (2006) 10380-10381.
- [22] H.J. Kim, C.H. Heo, H.M. Kim, *J. Am. Chem. Soc.* 135 (2013) 17969-17977.
- [23] S. Santra, S.K. Dogra, *Chem. Phys.* 226 (1998) 285-296.
- [24] J. Dey, S.K. Dogra, *J. Phys. Chem.* 98 (1994) 3638-3644.

- [25] A. Mishra, S. Chatterjee, G. Krishnamoorthy, J. Photochem. Photobiol. A-Chem., 260 (2013) 50-58.
- [26] S. Muhammad, H. Xu, M.R.S.A. Janjua, Z. Su, M. Nadeem, Phys. Chem. Chem. Phys., 12 (2010) 4791-4799.
- [27] Y.J. Li, T.F. Liu, H.B. Liu, M.Z. Tian, Y.L. Li, Accounts Chem. Res. 47 (2014) 1186-1198.
- [28] S.H. Kim, S.Y. Lee, S.Y. Gwon, Y.A. Son, J.S. Bae, Dyes Pigment. 84 (2010) 169-175.
- [29] B.K. An, J. Gierschner, S.Y. Park, Accounts Chem. Res. 45 (2012) 544-554.
- [30] B.K. An, S.K. Kwon, S.D. Jung, S.Y. Park, J. Am. Chem. Soc. 124 (2002) 14410-14415.
- [31] Y. Li, F. Li, H. Zhang, Z. Xie, W. Xie, H. Xu, B. Li, F. Shen, L. Ye, M. Hanif, D. Ma, Y. Ma, Chem. Comm. (2007) 231-233.
- [32] M.J. Percino, V.M. Chapela, M. Ceron, G. Soriano-Moro, M.E. Castro, F.J. Melendez, J. Mol. Struct. 1034 (2013) 238-248.
- [33] J. Mei, Y. Hong, J.W.Y. Lam, A. Qin, Y. Tang, B.Z. Tang, Adv. Mater. 26 (2014) 5429-5479.
- [34] V. Palakollu, S. Kanvah, New J. Chem. 38 (2014) 5736-5746.
- [35] P. Xue, B. Yao, J. Sun, Z. Zhang, K. Li, B. Liu, R. Lu, Dyes Pigment. 112 (2015) 255-261.
- [36] M. Hranjec, G. Pavlovic, G. Karminski-Zamola, Struct. Chem. 18 (2007) 943-949.
- [37] C. Reichardt, Chem. Rev. 94 (1994) 2319-2358.
- [38] A.V. Marenich, C.J. Cramer, D.G. Truhlar, J. Phys. Chem. B 113 (2009) 6378-6396.
- [39] I. Picek, R. Vianello, P. Sket, J. Plavec, B. Foretic, J. Org. Chem. 80 (2015) 2165-2173.
- [40] D. Saftić, R. Vianello, B. Žinić, Eur. J. Org. Chem. 2015 (2015) 7695-7704.
- [41] W.P. Jencks, J. Regenstein, Ionization Constants of Acids and Bases, in: Handbook of Biochemistry and Molecular Biology, Fourth Edition, CRC Press, 1976, pp. 305-351.

- [42] M.J. Frisch, G.W. Trucks, H.B. Schlegel, G.E. Scuseria, M.A. Robb, J.R. Cheeseman, G. Scalmani, V. Barone, B. Mennucci, G.A. Petersson, H. Nakatsuji, M. Caricato, X. Li, H.P. Hratchian, A.F. Izmaylov, J. Bloino, G. Zheng, J.L. Sonnenberg, M. Hada, M. Ehara, K. Toyota, R. Fukuda, J. Hasegawa, M. Ishida, T. Nakajima, Y. Honda, O. Kitao, H. Nakai, T. Vreven, J.A. Montgomery Jr., J.E. Peralta, F. Ogliaro, M.J. Bearpark, J. Heyd, E.N. Brothers, K.N. Kudin, V.N. Staroverov, R. Kobayashi, J. Normand, K. Raghavachari, A.P. Rendell, J.C. Burant, S.S. Iyengar, J. Tomasi, M. Cossi, N. Rega, N.J. Millam, M. Klene, J.E. Knox, J.B. Cross, V. Bakken, C. Adamo, J. Jaramillo, R. Gomperts, R.E. Stratmann, O. Yazyev, A.J. Austin, R. Cammi, C. Pomelli, J.W. Ochterski, R.L. Martin, K. Morokuma, V.G. Zakrzewski, G.A. Voth, P. Salvador, J.J. Dannenberg, S. Dapprich, A.D. Daniels, Ö. Farkas, J.B. Foresman, J.V. Ortiz, J. Cioslowski, D.J. Fox, Gaussian 09, in, Gaussian, Inc., Wallingford, CT, USA, 2009.
- [43] V.K. Gupta, A.K. Singh, L.K. Kumawat, *Sens. Actuator B-Chem.* 195 (2014) 98-108.
- [44] H. Auweter, H. Haberkorn, W. Heckmann, D. Horn, E. Luddecke, J. Rieger, H. Weiss, *Angew. Chem.-Int. Edit.* 38 (1999) 2188-2191.
- [45] J. Luo, Z. Xie, J.W.Y. Lam, L. Cheng, H. Chen, C. Qiu, H.S. Kwok, X. Zhan, Y. Liu, D. Zhu, B.Z. Tang, *Chem. Comm.* (2001) 1740-1741.
- [46] F. Würthner, *Accounts Chem. Res.* 49 (2016) 868-876.
- [47] Y.P. Li, F. Li, H.Y. Zhang, Z.Q. Xie, W.J. Xie, H. Xu, B. Li, F.Z. Shen, L. Ye, M. Hanif, D.G. Ma, Y.G. Ma, *Chem. Comm.* (2007) 231-233.
- [48] U. Rösch, S. Yao, R. Wortmann, F. Würthner, *Angew. Chem.* 118 (2006) 7184-7188.
- [49] R. Vianello, Z.B. Maksic, *New J. Chem.* 33 (2009) 739-748.
- [50] R. Vianello, Z.B. Maksic, *J. Org. Chem.* 75 (2010) 7670-7681.
- [51] X. Xie, E. Bakker, *Anal. Bioanal. Chem.* 407 (2015) 3899-3910.

[52] M. Hranjec, G. Pavlović, M. Marjanović, M. Kralj, G. Karminski-Zamola, Eur. J. Med. Chem. 45 (2010) 2405-2417.

ACCEPTED MANUSCRIPT

Figure captions

Fig. 1. D- π -A molecular system based on benzimidazole derivative.

Fig. 2. Synthesised benzimidazole derivatives **1-4**.

Fig. 3. D- π -A arrangement and protonable – deprotonable sites of (a) **3** and (b) **4**.

Fig. 4. Absorption spectra of compounds **1-4**, $c = 1 \times 10^{-5}$ M, in (a) ethanol and (b) water.

Fig. 5. (a) Absorbance and emission spectra of compound **3** in water and in ethanol, $\lambda_{exc} = 350$ nm; (b) Absorbance of **3** in ethanol/water mixtures recorded at 425 nm; (c) Photographs of **3** in water/ethanol mixtures under ambient light and under UV lamp (365 nm), volume fraction of ethanol in mixed solutions, $f_{EtOH} = 0 - 40\%$, $c(\mathbf{3}) = 1 \times 10^{-5}$ M.

Fig. 6. Absorption and emission spectra of compounds **1 - 4**, $c = 1 \times 10^{-5}$ M, in neutral and protonated form in ethanol. (Excitation wavelength at absorption maximum of corresponding species.)

Scheme 1. General scheme of acid-base equilibria **1-4**.

Fig. 7. Spectroscopic pH titration of (a) **3** and (b) **4**, $c = 1 \times 10^{-5}$ mol dm⁻³ in aqueous solutions and corresponding equilibria.

Fig. 8. Absorbance data plotted versus pH for (a) **3** and (b) **4** at selected wavelengths.

Fig. 9. (a) Absorbance spectra of chromophore **3** immobilised in plasticised PVC film at different pH values; (b) calibration plot of immobilised chromophore **3** (absorbance change in response to pH at 495 nm).

Fig. 10. a) Absorption and b) emission spectra ($\lambda_{exc} = 350$ nm) of **3** in aqueous solution (buffer pH = 7.0) upon titration with DNA.

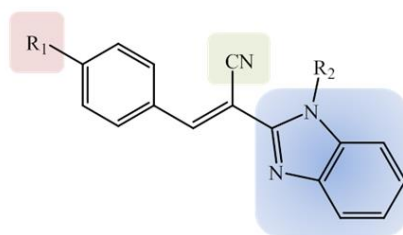


Fig. 1

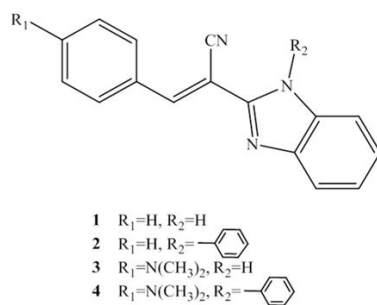


Fig. 2

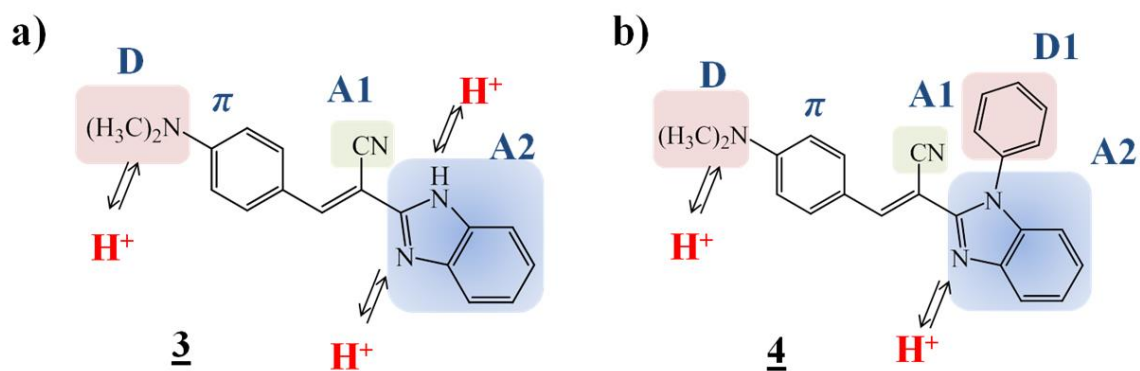


Fig. 3

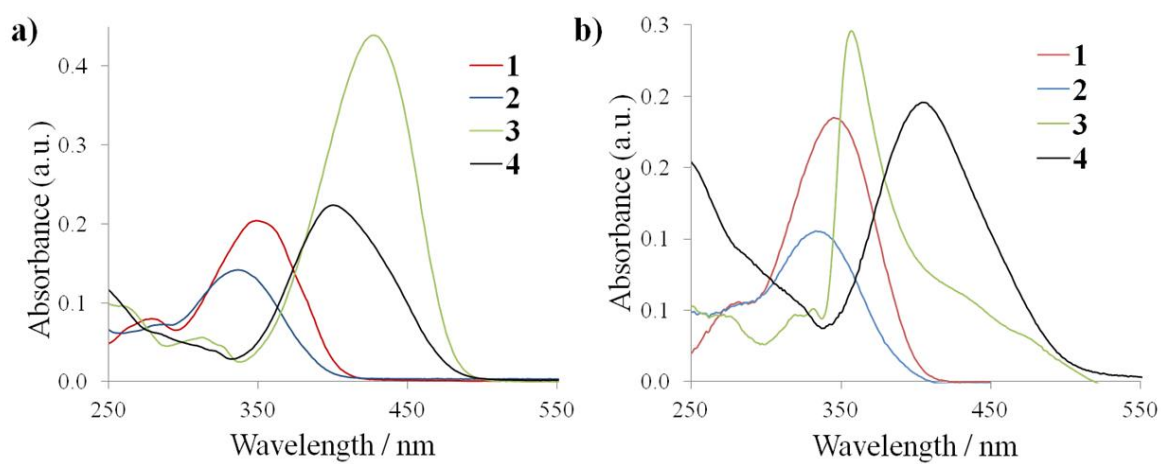


Fig. 4

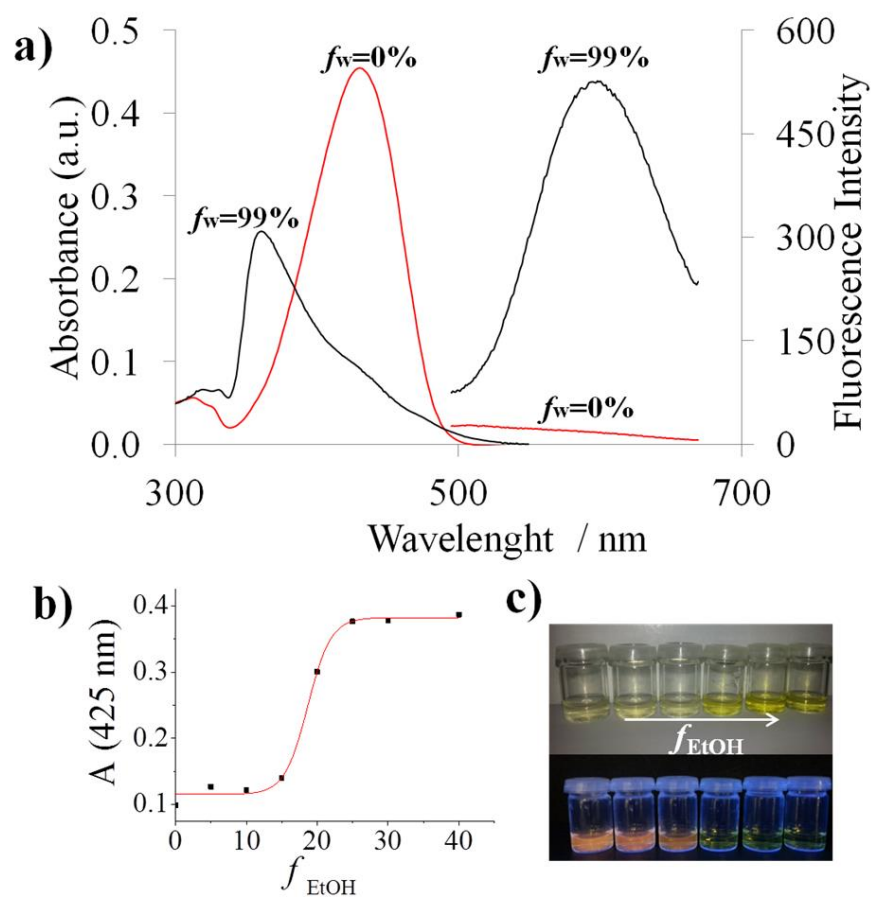


Fig. 5

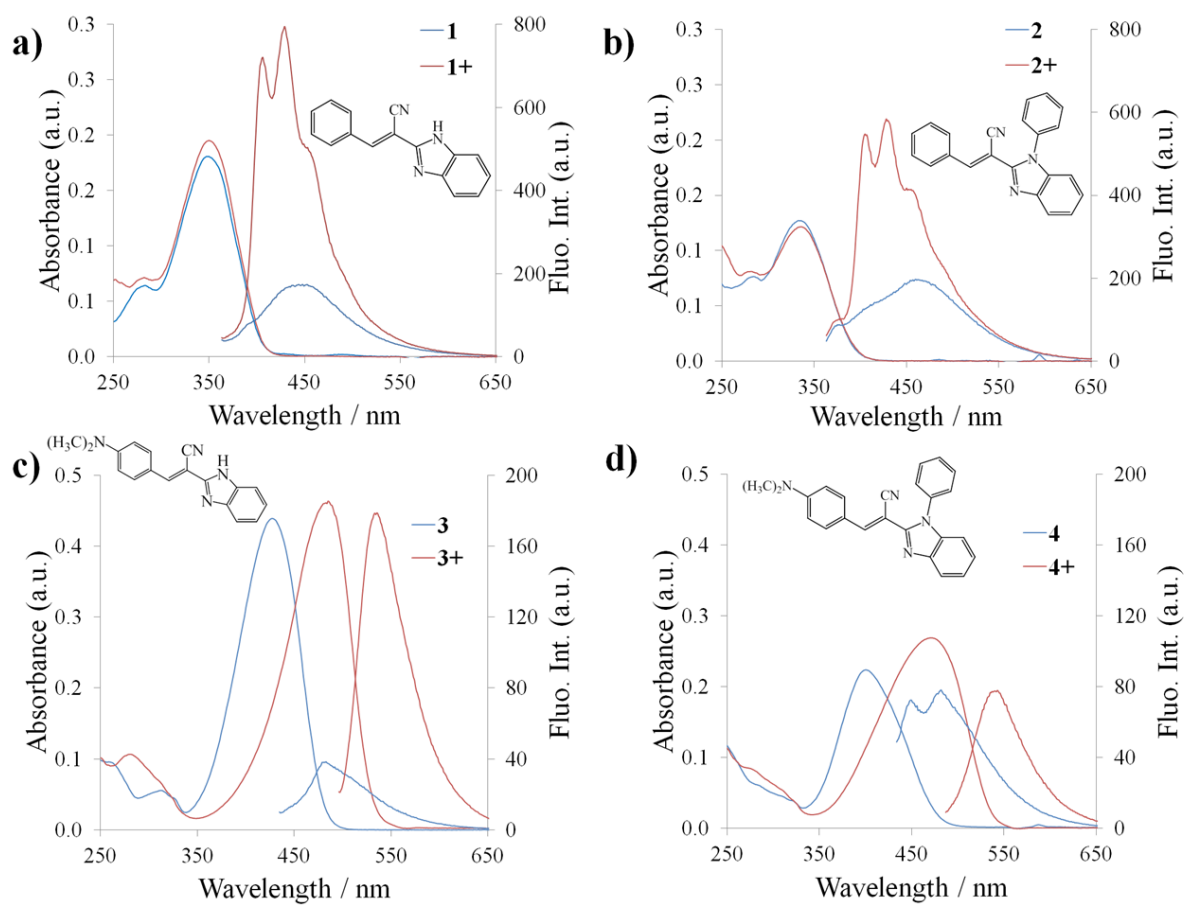


Fig. 6

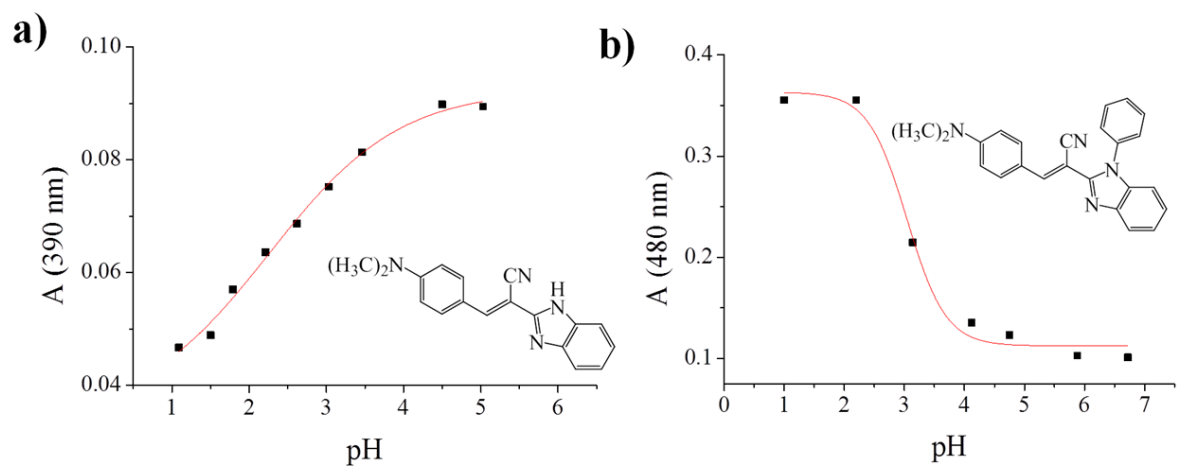


Fig. 8

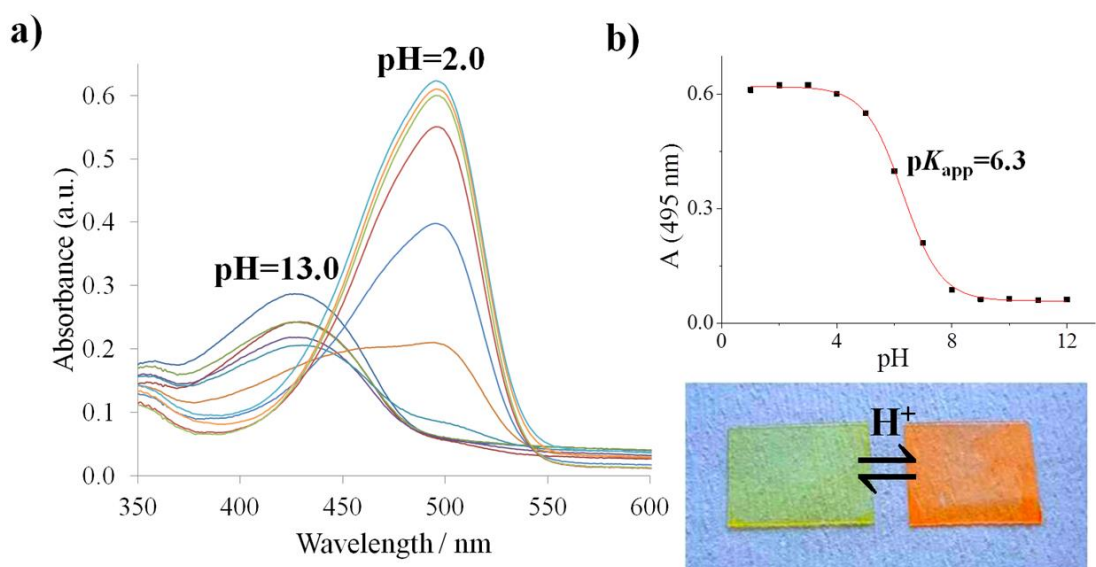


Fig. 9

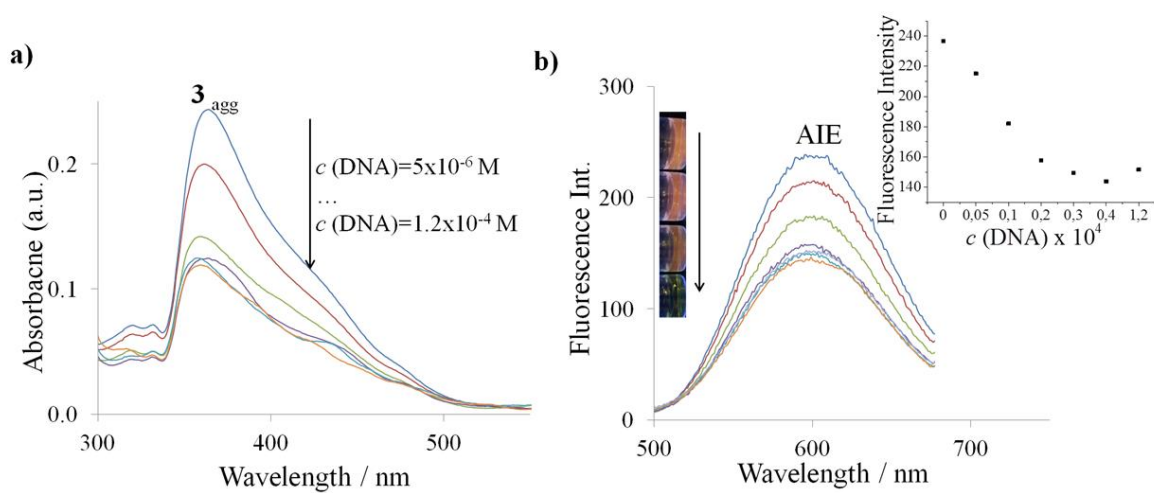
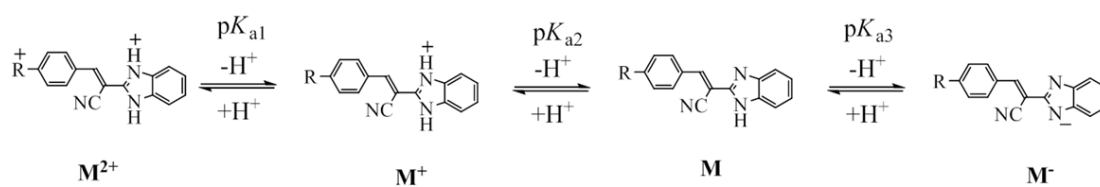


Fig. 10



Scheme 1

Table 1. Photophysical properties of compounds **1-4** in ethanol.

Compound	Absorption		Emission		
	$\lambda_{abs} /$ nm	$\varepsilon \times 10^{-3} /$ $M^{-1}cm^{-1}$	$\lambda_{em} /$ nm	Stokes shift / nm	Φ
1	204	20.40	444	100	0.0027
	<u>350^a</u>				
2	202	14.13	464	136	0.0045
	<u>335</u>				
3	202	43.91	491	66	0.0021
	<u>425</u>				
4	202	22.38	486	86	0.0022
	<u>400</u>				

^aunderlined values were used to calculate molar absorption coefficients and Stokes shifts

Table 2. Maximum absorbance wavelengths, molar absorption coefficients and FWHM values of benzimidazole chromophores in solvents of different polarities and $E_T(30)$ values.

Comp.		Solvent ^a				
		Toluene $E_T(30)=33.9$	Ethyl acetate $E_T(30)=38.1$	EtOH $E_T(30)=51.9$	MeOH $E_T(30)=55.4$	H ₂ O $E_T(30)=63.1$
1	λ_{abs} (nm)	362	350	350	346	344
	$\varepsilon \times 10^{-3}$ (M ⁻¹ cm ⁻¹)	20.12	24.23	20.40	22.27	17.87
	FWHM (nm)	72	70	73	70	70
2	λ_{abs} (nm)	345	343	335	334	335
	$\varepsilon \times 10^{-3}$ (M ⁻¹ cm ⁻¹)	28.23	32.97	14.13	27.11	10.56
	FWHM (nm)	70	71	65	69	63
3	λ_{abs} (nm)	430 (48.42)	420	425	425	356
	$\varepsilon \times 10^{-3}$ (M ⁻¹ cm ⁻¹)	48.42	42.01	43.91	38.09	24.58 ^b
	FWHM (nm)	77	75	86	81	33 ^b
4	λ_{abs} (nm)	390	390	400	400	404
	$\varepsilon \times 10^{-3}$ (M ⁻¹ cm ⁻¹)	30.42	25.87	22.38	32.42	19.61
	FWHM (nm)	59	64	68	64	89

^a solvents contained 1 % of ethanol (volume fraction of ethanol, $f_{EtOH}=1\%$), ^baggregation

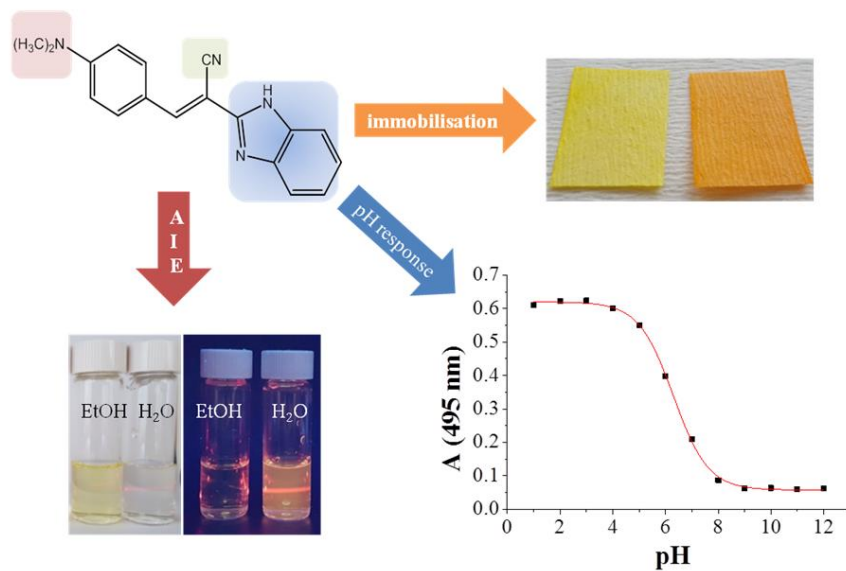
Table 3. Experimentally estimated and theoretically calculated pK_a values in water.

Compound	Acid-base equilibria	pK_a	pK_a
		($I = 0,1M$)	calculated
1	$\mathbf{1}^+ \rightleftharpoons \mathbf{1} + \text{H}^+$	$pK_{a2}=2.7$	$pK_{a2}=3.0$
	$\mathbf{1} \rightleftharpoons \mathbf{1}^- + \text{H}^+$	$pK_{a3}>10.3$	$pK_{a3}=10.4$
2	$\mathbf{2}^+ \rightleftharpoons \mathbf{2} + \text{H}^+$	$pK_{a2}=2.5$	$pK_{a3}=2.4$
3	$\mathbf{3}^{2+} \rightleftharpoons \mathbf{3}^+ + \text{H}^+$	$pK_{a1}<1.5$	$pK_{a1}=1.1$
	$\mathbf{3}^+ \rightleftharpoons \mathbf{3} + \text{H}^+$	$pK_{a2}=2.2^a$	$pK_{a2}=4.2$
	$\mathbf{3} \rightleftharpoons \mathbf{3}^- + \text{H}^+$	$pK_{a3}>10.4^a$	$pK_{a3}=10.3$
4	$\mathbf{4}^{2+} \rightleftharpoons \mathbf{4}^+ + \text{H}^+$	$pK_{a1}<1.5$	$pK_{a1}=2.0$
	$\mathbf{4}^+ \rightleftharpoons \mathbf{4} + \text{H}^+$	$pK_{a2}=3.0$	$pK_{a2}=3.7$
I	$\mathbf{I}^{2+} \rightleftharpoons \mathbf{I}^+ + \text{H}^+$	$pK_{a1}=3.4^b$	$pK_{a1}=3.3$
	$\mathbf{I}^+ \rightleftharpoons \mathbf{I} + \text{H}^+$	$pK_{a2}=6.0^b$	$pK_{a2}=5.8$
	$\mathbf{I} \rightleftharpoons \mathbf{I}^- + \text{H}^+$	-	$pK_{a3}=12.5$

^aaggregation in aqueous solution

Table 4. Absorption maxima, emission maxima and apparent pK_a values of neutral and monocation form of **3** and **4** immobilised in thin polymer films.

Compound	$\lambda_{\text{abs}}/\text{nm}$	$\lambda_{\text{em}}/\text{nm}$	$\lambda_{\text{abs}}/\text{nm}$	$\lambda_{\text{em}}/\text{nm}$	pK_a
	M	M	M⁺	M⁺	apparent
3	428	494	495	544	6.30
4	400	481	490	548	6.32



Graphical abstract

Highlights

- Benzimidazole based acrylonitriles synthesised as push-pull chromophores
- Compound **3** shows aggregation induced emission (AIE) at 600 nm in aqueous solutions
- Structure-property study of pH sensitivity and pK_a values of chromophores in aqueous solutions
- pH sensitive polymeric materials with the apparent pK_a values of around 6